

## Contents

<b>1</b>	<b>Introduction</b>	<b>1</b>
<b>2</b>	<b>Green Bank Site Weather Data</b>	<b>5</b>
<b>3</b>	<b>Noise vs Saturation Power</b>	<b>9</b>
<b>4</b>	<b>Total Statistical Weight of the Data vs Saturation Power</b>	<b>10</b>
<b>5</b>	<b>Other Considerations</b>	<b>13</b>
	5.1 Stability . . . . .	13
	5.2 High Load Observing . . . . .	13
<b>6</b>	<b>Saturation Risk Mitigation Strategies</b>	<b>13</b>
<b>7</b>	<b>Summary &amp; Conclusions</b>	<b>14</b>

## 1 Introduction

In this memo we consider the saturation power specification for the MUSTANG-2 detectors and the impact that this specification has on the total system noise on the sky, in practice, considering the range of useful 90 GHz observing conditions at the Green Bank site. Expressions for the bolometer photon noise, phonon noise, etc. are taken from Mather (1982), Richards (1994), and Sayers (2008). We assume response to only a single polarization.

The sensitivity of an ideal, single-polarization bolometric detector is limited<sup>1</sup> by the noise of the input radiation field

$$NEP_{BLIP}^2 = NEP_{poisson}^2 + NEP_{Bose}^2 \quad (1)$$

$$= 2h\nu_o\eta\epsilon k_B T \Delta\nu + 2(\eta\epsilon k_B T \Delta\nu)^2 / \Delta\nu \quad (2)$$

$$= 2h\nu_o Q + 2Q^2 / \Delta\nu \quad (3)$$

where  $T$  is the physical temperature of the background (here assumed to be all sky  $\sim 265$  K),  $\epsilon$  is the emissivity of the background ( $\sim 0.1$ ),  $\eta$  is the optical

---

<sup>1</sup>The photon noise-limited situation is often called Background Limited Performance (BLIP).

efficiency measured from the background source to the detector, and  $\nu_o$  is the center of a square band  $\Delta\nu$ .  $Q$  is the total optical loading,

$$Q = \eta\epsilon k_B T \Delta\nu \quad (4)$$

Since  $n\nu_o/k_B T \ll 1$  we have assumed the Rayleigh-Jeans approximation for the background radiation field. The Bose term in the above equation gives rise to the familiar radiometer equation at low frequencies (when  $\nu_o < \eta\epsilon k_B T/h$ ), and the Poisson term gives rise to the shot noise which typically dominates at millimeter and submillimeter wavelengths.

A real detector must contend with the intrinsic thermal noise fluctuations arising from phonons which carry heat from the detector the thermal bath, often called phonon noise or G-noise. For a detector at temperature  $T_c$ , this is given by

$$NEP_G^2 = 4k_B T_c^2 G_c F_{link} \quad (5)$$

where  $G_c$  is the *thermal conductance* (in units of Watts/Kelvin) between the detector and the thermal bath, at an assumed<sup>2</sup> temperature  $T_o$ .  $G_c$  is often (confusingly) called the thermal conductivity, although thermal conductivity conventionally has units of power/temperature/length. In general it is a function of temperature, at low temperature parameterizable as

$$G(T) = G_c \left( \frac{T}{T_c} \right)^{N-1}. \quad (6)$$

For our devices  $N - 1 \sim 1.8$ .  $F_{link}$  is a dimensionless factor depending on the material properties, given by

$$F_{link}(T) = \frac{1}{2} (1 + (T_o/T)^{N+1}) \quad (7)$$

A TES detector must be maintained at its transition temperature  $T_c > T_o$ , and there is some power loading  $P_{sat}$  which does this. This can be shown to be

$$P_{sat} = \frac{G_c T_c}{N} (1 - (T_o/T_c)^N) \quad (8)$$

If the incident optical+ohmic loading is higher than this the TES detectors will be non-responsive. The highest desired operational optical loading therefore determines the design goal for the detector  $G$ ,

$$G_c \equiv G(T_c) = \frac{P_{sat}}{T_c} \frac{N}{1 - (T_o/T_c)^N} \quad (9)$$

This therefore determines the total phonon noise via Eq. 5

$$NEP_G = \sqrt{2k_B T_c P_{sat} \frac{N(1 + (T_o/T_c)^{N+1})}{1 - (T_o/T_c)^N}} \quad (10)$$

<sup>2</sup>Unless otherwise specified all calculations in this memo assume  $T_c = 490$  mK and  $T_o = 300$  mK.

$P_{sat}$  is given by

$$P_{sat} = \kappa \eta_{design} \epsilon_{worst} k_B T \Delta\nu + P_{instr} \quad (11)$$

here  $\eta_{design}$  is the design goal for the system optical efficiency which is assumed in the saturation power calculation, and  $\epsilon_{worst}$  is the highest atmospheric emissivity under which it is desirable to collect useful data (including the airmass factor  $A$ ).  $\kappa$  is a “safety factor”, typically chosen to have a value  $\sim 2$ , to allow a margin of error in the design calculations.  $P_{instr}$  is the instrumental loading, estimated to be 5 pW. For realistic values

$$P_{sat} = \kappa \times \left[ 21.5 \text{ pW} \times \left( \frac{\eta_d}{65\%} \right) \left( \frac{\epsilon_{worst} T}{2 \times 40\text{K}} \right) \left( \frac{\Delta\nu}{30\text{GHz}} \right) + 5 \text{ pW} \right] \quad (12)$$

Then the ratio of G-noise to photon background noise is

$$\frac{NEP_G}{NEP_{BLIP}} = \sqrt{\frac{\eta_{design} \epsilon_{worst}}{\eta \epsilon} \frac{k_B T_c}{h\nu_o + \eta \epsilon k_B T} \frac{N(1 + (T_o/T_c)^{N+1})}{1 - (T_o/T_c)^N}} \quad (13)$$

Here  $\epsilon_{worst}/\epsilon$  is the required dynamic range in total power. For a useful, general-purpose millimeter or submillimeter instrument this will be at least a factor of 2 – 3. The ratio of G-noise to background photon noise is plotted for 3 different precipitable water vapor (PWV) column densities in Figure 1. The sky brightness is calculated using ATM (Pardo 2001). With realistic design tolerancing the phonon noise and photon noise are comparable at 100 GHz under the very best sky conditions (and at zenith), motivating a careful consideration of the saturation specification. At higher frequencies achieving BLIP is easier due to the increased photon noise.

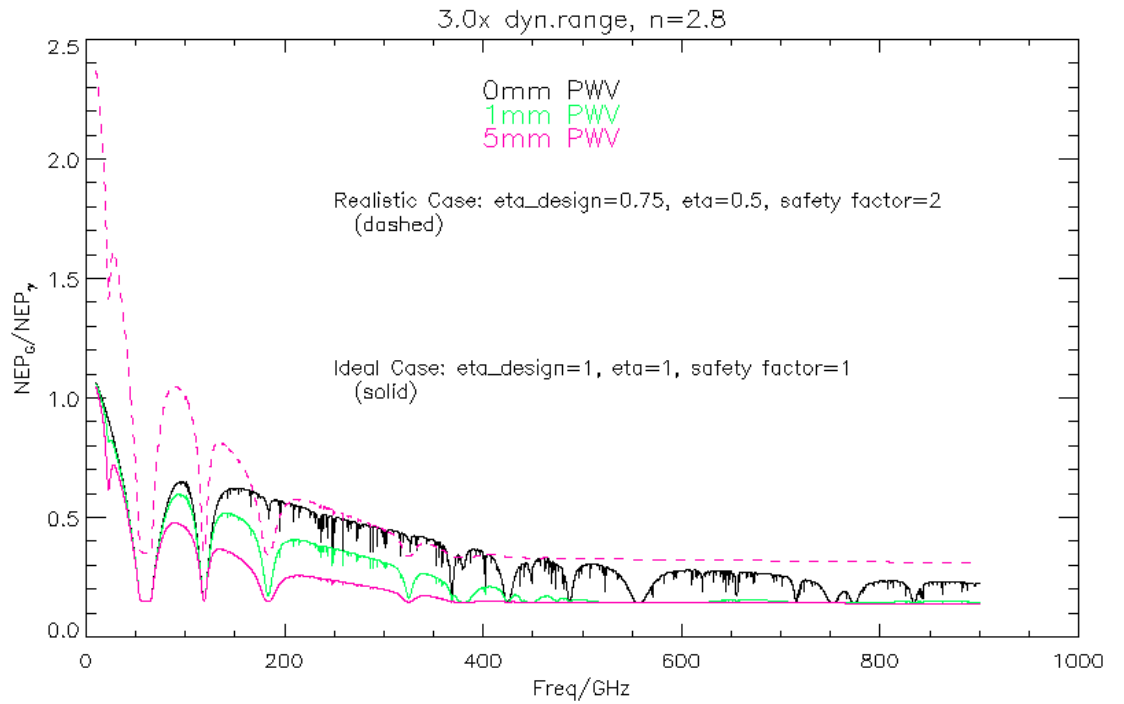


Figure 1: Ratio of phonon noise to photon noise vs. frequency for ideal (no safety factor, perfect assumed & achieved optical efficiency; for  $T_c = 490$  mK,  $T_o = 300$  mK) and realistic cases, for 0 mmm, 1 mm, and 5 mm PWV. For all cases the photon noise is calculated at zenith, and the saturation power is set under the given conditions at 30 degrees elevation allowing  $1.5 \times \kappa$  additional overhead in total power.

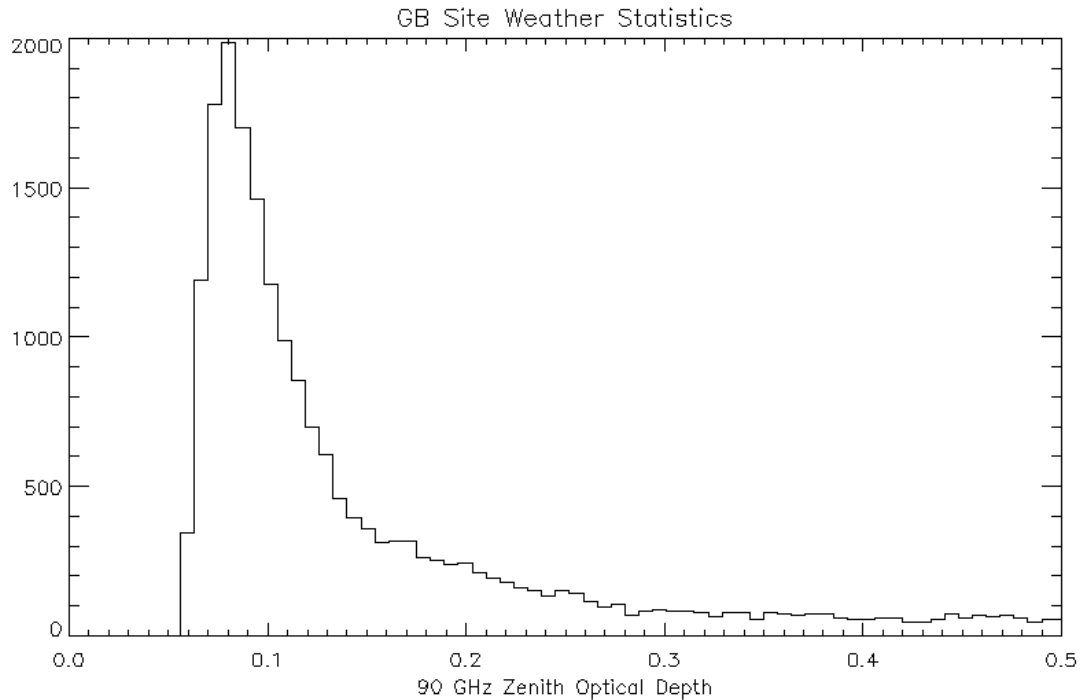


Figure 2: Distribution of 90 GHz atmospheric optical depth at zenith in Green Bank.

## 2 Green Bank Site Weather Data

Sophisticated models of the microwave properties of the atmosphere have been developed by Ron Maddalena<sup>3</sup> making use of National Weather Service vertical profile models. We have retrieved archival values of the 90 GHz atmospheric brightness temperature, opacity, and vertically averaged thermodynamic temperature for the period 2004 - 2009. These are shown in Figures 2 - 5. Each datum represents a single hour.

---

<sup>3</sup>see <http://www.gb.nrao.edu/~rmaddale/Weather/index.html>

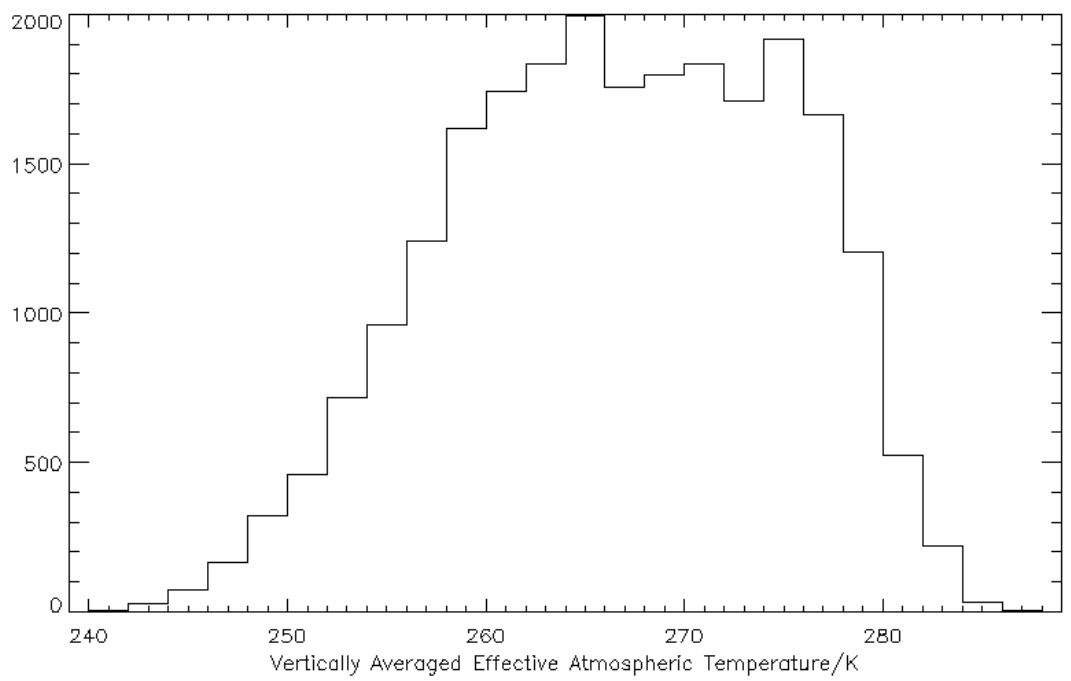


Figure 3: Vertically averaged atmospheric thermodynamic temperature.

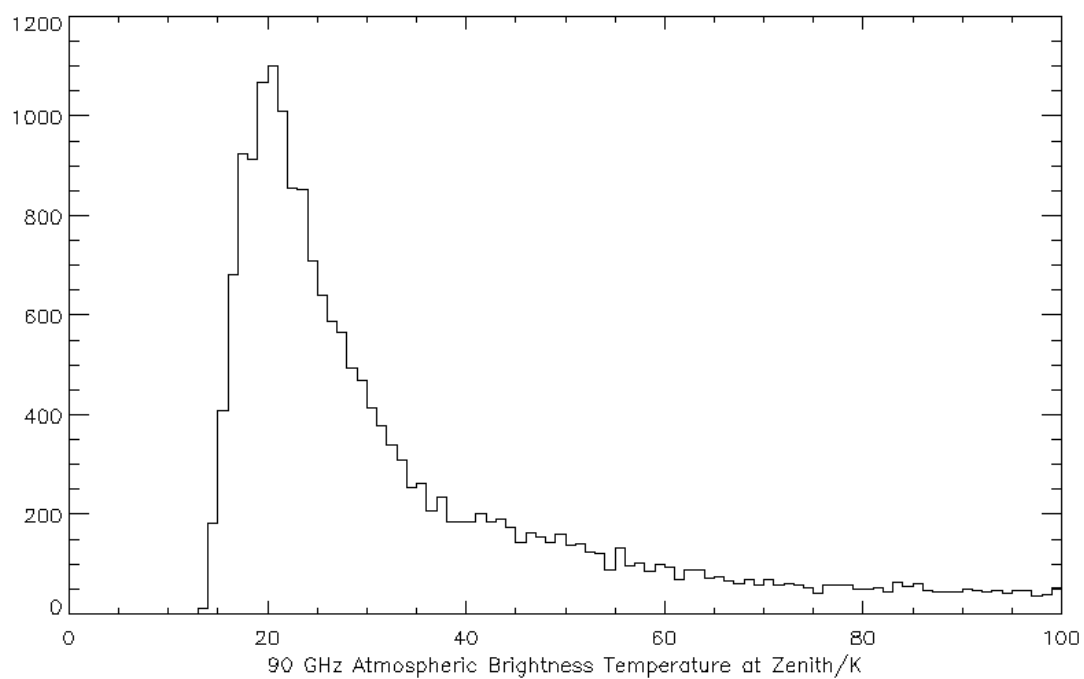


Figure 4: Distribution of 90 GHz atmospheric brightness temperature at zenith in Green Bank.

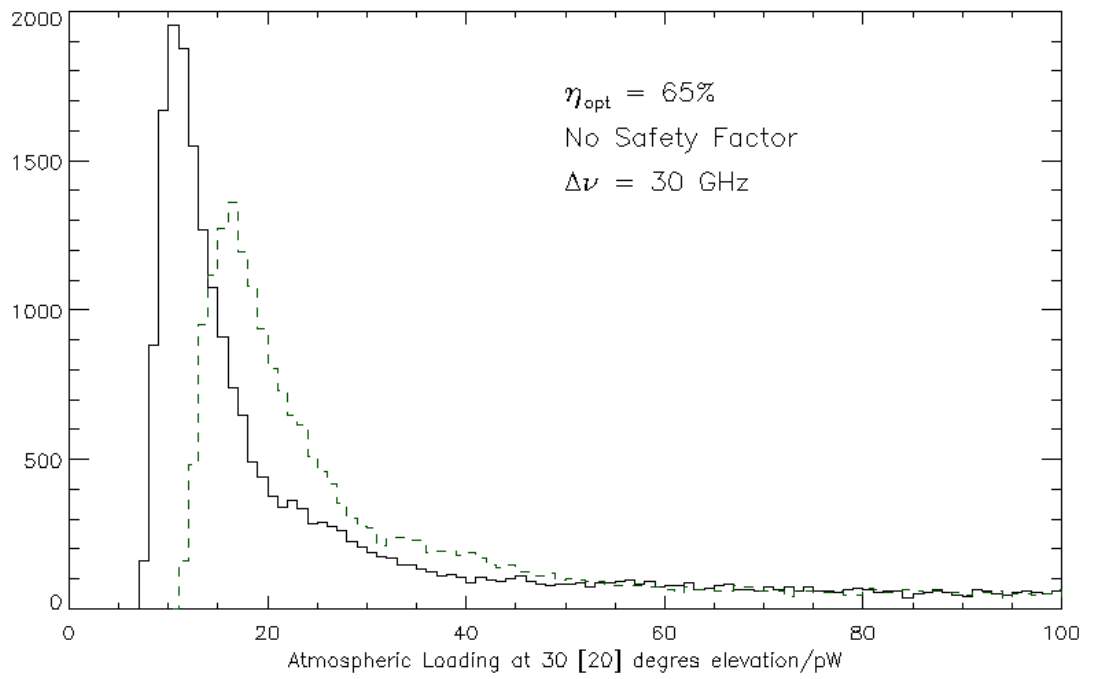


Figure 5: Distribution of 90 GHz atmospheric loading at 30 and 20 degrees elevation in Green Bank, computed from the zenith brightness temperature in Figure 4.

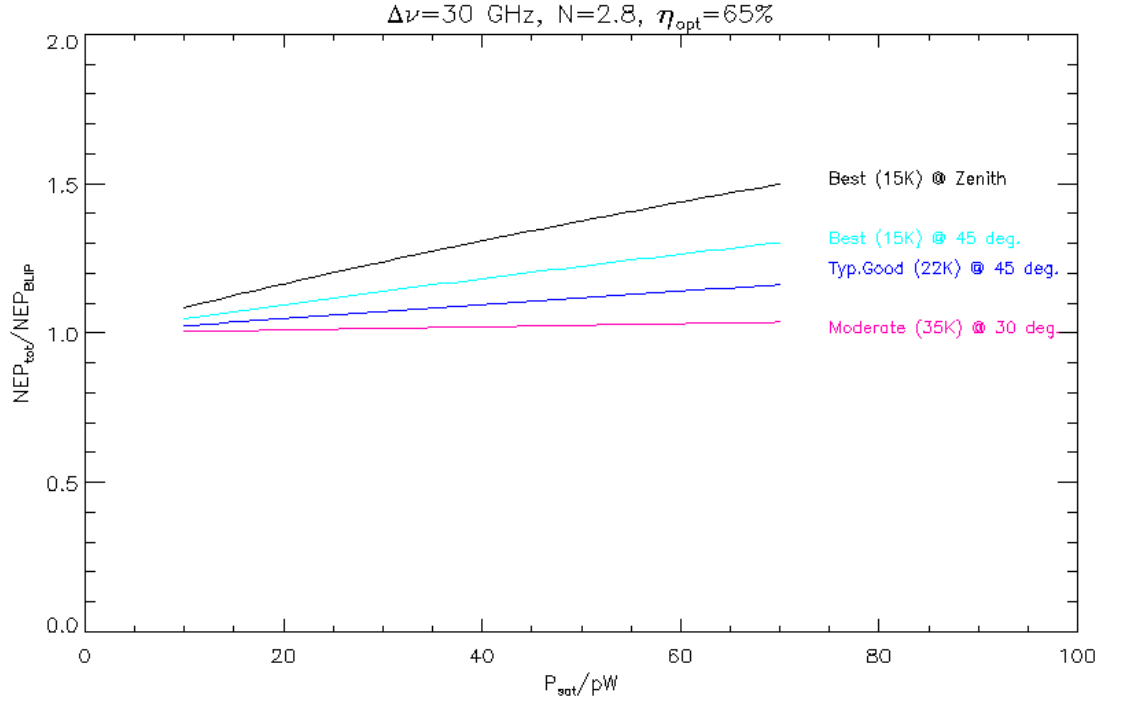


Figure 6: Total noise as a function of saturation power for a range of observing conditions.

### 3 Noise vs Saturation Power

For a given sky loading the total detector plus sky noise is

$$NEP_{\text{tot}} = \sqrt{NEP_G^2 + NEP_{\text{BLIP}}^2} \quad (14)$$

using Eqs. 10 and 3 for the photon and G-noise. This is shown as a function of saturation power for a range of representative observing conditions in Figure 6.

## 4 Total Statistical Weight of the Data vs Saturation Power

To quantify the tradeoff between photon noise and integration time we consider a series of integrations equal in duration, on a single point on the sky, with an assumed, fixed airmass  $A$ .  $P_{sat}$  and therefore  $NEP_G$  are given. For integration  $i$  the opacity is  $\tau_i$  and the noise is  $NEP_{tot,i} = \sqrt{NEP_G^2 + NEP_{BLIP,i}^2}$ , with  $NEP_{BLIP,i}$  computed from the weather at the time of the integration. The total signal to noise obtained is then proportional to

$$S = \left( \sum_i^{P_i < P_{sat}} \frac{e^{-2\tau_i A}}{NEP_{tot,i}^2} \right)^{1/2} \quad (15)$$

where  $P_i$  is the total loading at 30 degrees elevation for the weather at integration  $i$ :

$$P_i = \kappa \eta_{design} A_{sat} \epsilon_i k_B T_i \Delta\nu + P_{instr} \quad (16)$$

where  $T_i$  is the 90 GHz brightness temperature of the atmosphere at zenith. While we require that it be possible to observe down to 30 degrees elevation ( $A_{sat} = 2$ ) for data collected in each weather period to be useful, the actual sensitivity optimization is carried out at the more representative value of  $A = 1.4$  (45 degrees elevation).

The fraction of usable time by this criterion, including 5 pW instrument + ground loading, and using the  $\tau$  and  $T_{90}$  distributions for the GB site (§2) is shown in Figure 7. (note that this does not include wind or day/night constraints, which do not substantially alter the distribution)

The distribution of this total SNR proxy  $S$  is shown in Figure 8. It is notable that the falloff from the optimum is much slower on the high-power side than the low-power side, indicating that a “conservative” choice of  $P_{sat}$  gives rise to only a modest penalty in system performance. This analysis indicates that a saturation power of 29 pW gives an optimum compromise between sensitivity and useful integration time. Since our loading is dominated by the atmosphere, and since there are good options for mitigating the risk of saturation (§ 6), we adopt a relatively aggressive safety factor  $\kappa \sim 1.5$  and a target  $P_{sat} = 45$  pW.

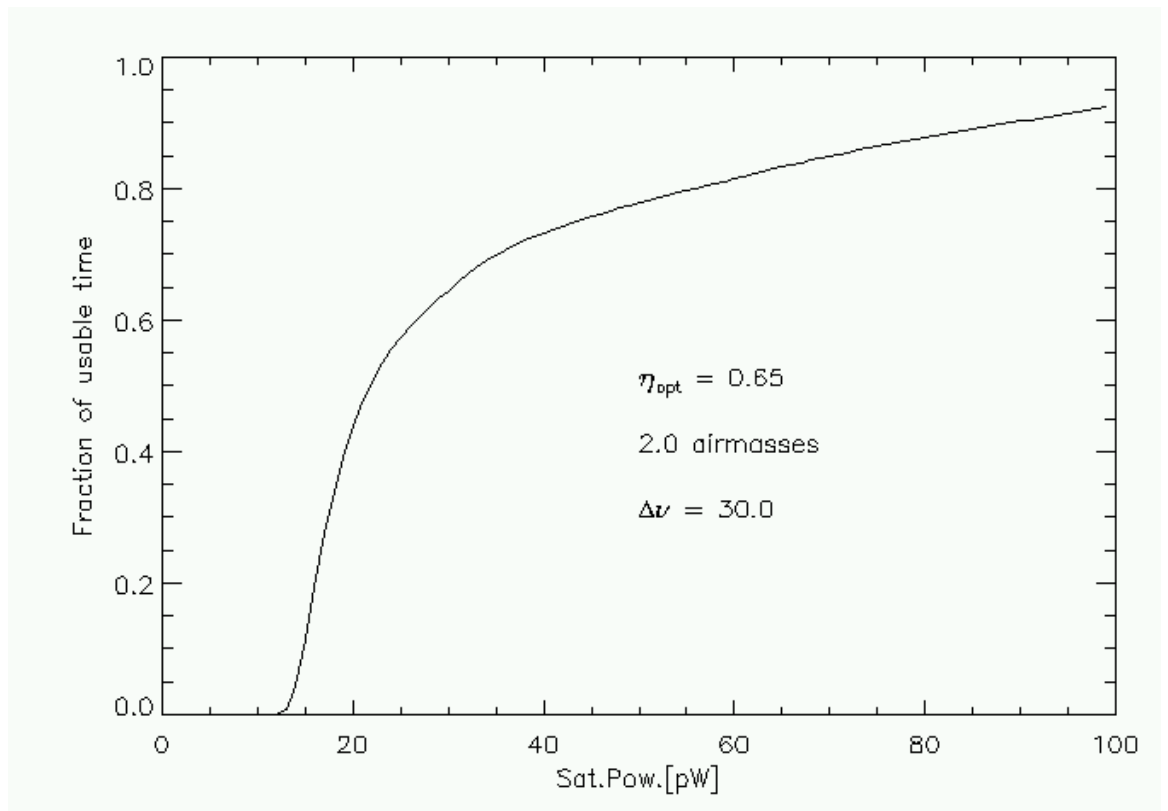


Figure 7: Fraction of usable data, including 5 pW instrument and ground loading; not allowing for additional day/night and wind cuts. No safety factor is included.

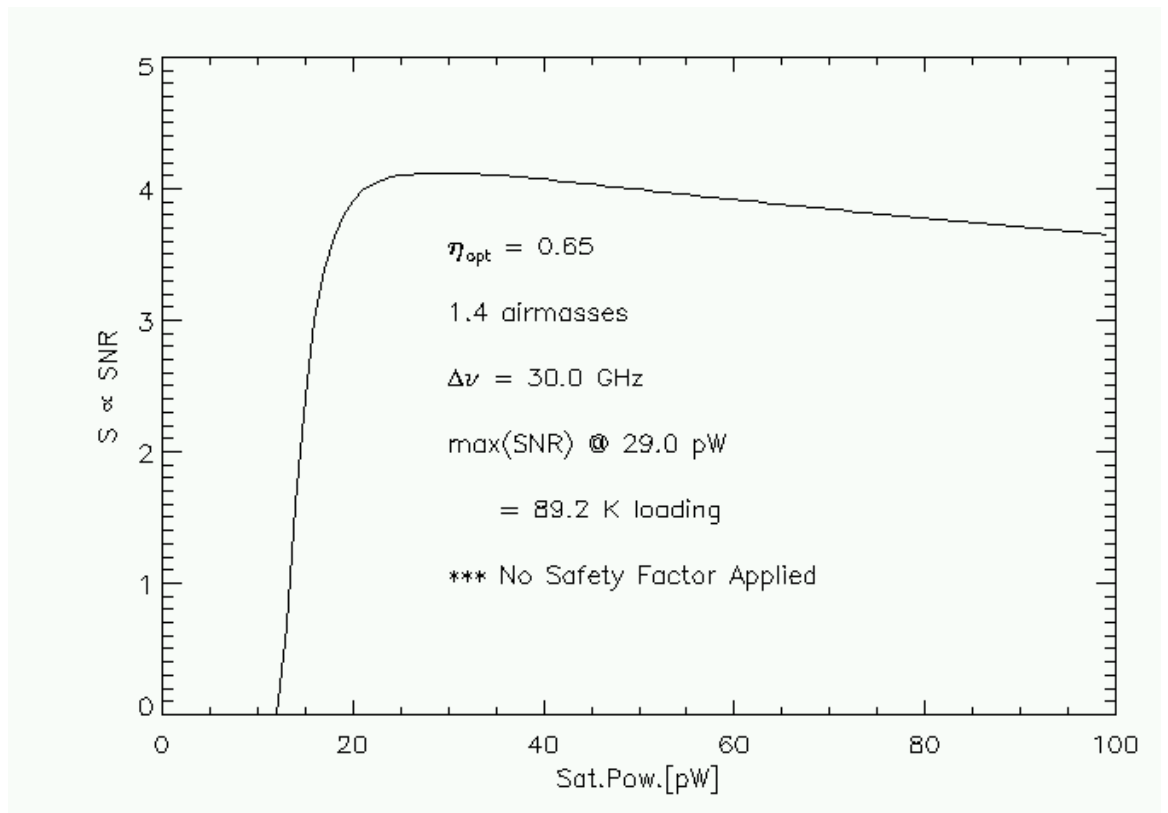


Figure 8: Total statistical power  $S$  (as defined above) as a function of saturation power.

## 5 Other Considerations

### 5.1 Stability

This analysis considers only idealized, statistically stationary noise sources. In practice, fluctuations in atmospheric water vapor along the line of sight are often a limiting factor. Previous analysis of MUSTANG data (GBT Memo 269) has found: i) the best, most stable conditions occur when the sky brightness on the line of sight (including airmass effects) is less than 40 K; ii) usable conditions occur > 85% of the time when the line of sight brightness temperature is 80K or less. For  $\eta = 65\%$  these correspond to 10.8 pW and 21.5 pW. Including the 5pW instrument loading and a 1.5 safety factor these on their own would suggest  $P_{sat} = 21$  pW and 40 pW, respectively.

### 5.2 High Load Observing

While most MUSTANG-2 observing will be done under the best weather and the lowest loading conditions possible, some scientifically interesting objects lie at low declinations, requiring observing through several airmasses of atmosphere. Some objects are located at right ascensions requiring observing at non-optimal times of year, since the GBT 3mm performance is only currently good at night due to dynamic thermal deformations of the structure.

A worst case is the Galactic Center, which is only observable at night from May onward into the summer and transits at 27° elevation. In May and June, suitable observing conditions exist for 19 hours total, on average (90 GHz brightness temperature due to the atmosphere at zenith is < 50 K; night-time; winds under 10mph). Supposing observations at 20° elevation with 50 K zenith brightness and no safety factor, the total loading would be 45 pW. This might be just possible but leaves no margin for error. Designing for this load would imply  $P_{sat} = 68$  pW, which would result in an unacceptable degradation of sensitivity under more typical, good-weather conditions, particularly if the achieved optical efficiency were to be considerably below the design goal.

A better option for scientifically interesting high-load observations is to reduce the loading by installing partially-reflective optical elements. This option is evaluated in the next section (§ 6).

## 6 Saturation Risk Mitigation Strategies

The detector saturation specification must balance two competing considerations: detector noise (which is lower for lower saturation powers), and available integration time / the risk of unexpectedly saturating the detectors (both of which favor higher saturation powers). One concern, for instance, is that there could be an unexpected load on the detectors which causes them to be saturated under all practical conditions. The optimal compromise and the resulting overall system sensitivity depends on the assumed receiver optical efficiency, while

in practice there may be some variance between the target and achieved optical efficiency.

We evaluated several strategies to deal with this risk:

1. Baseline: 92K saturation condition (80K+12K instrument and ground); 30 GHz bandpass,  $\eta_{design} = 65\%$ ,  $\eta_{achieved} = 65\%$ ,  $\kappa = 1.5$  ( $P_{sat}=40$  pW).
2. Realistic: same as 1 but  $\eta_{achieved} = 50\%$ .
3. NDF: extra 30K loading, compensate by reducing optical efficiency to  $\eta_{achieved} = 65\% \times (80/110) = 47\%$
4. lower BP: extra 30K loading, compensate by reducing bandwidth to 21.8 GHz
5. higher  $P_{sat}$ : extra 30K loading, compensate by designing for the higher loading level

Table 1 compares the SNR proxy  $\eta_{achieved}\Delta\nu/NEP_{tot}$  for these approaches.

In order of preference, the best strategies for dealing with extra loading are: 1) design for it (case 5); 2) add a neutral density filter; 3) reduce the optical bandpass. The differences between these strategies are modest (7% in sensitivity).

The option of dynamically reconfigurable (hence warm) reflective elements is appealing to easily enable a wider range of science targets (§ 5.2). A remotely openable radome with a suitably chosen material could serve this function, as could a warm neutral density filter.

Approach	$NEP_{\gamma}/10^{-17}$ [watts/ $\sqrt{\text{Hz}}$ ]	$NEP_G/10^{-17}$ [watts/ $\sqrt{\text{Hz}}$ ]	$NEP_{tot}/10^{-17}$ [watts/ $\sqrt{\text{Hz}}$ ]	$\eta\Delta\nu/NEP_{tot}$ [arb.]
1- Baseline	7.46	4.75	8.84	1.13
2- Realistic	5.89	4.75	7.57	1.02
3- NDF	10.4	4.75	11.43	0.63
4- Lower BP	12.0	4.75	12.90	0.60
5- Higher $P_{sat}$	14.1	5.43	15.10	0.64

Table 1: Comparison of saturation risk mitigation strategies.

## 7 Summary & Conclusions

Using archival weather data and atmospheric emission models, we have calculated the range of atmospheric optical loadings under useful 90 GHz observing conditions in Green Bank, finding typical loadings of 10–20 pW for  $\eta = 65\%$  and  $\Delta\nu = 30$  GHz. A formal optimization of total system performance, including the predicted ground and instrument loading, gives  $P_{sat} = 29$  pW, and show a weak degradation in system performance with increasing  $P_{sat}$ . A criterion

based on atmospheric stability gives similar results ( $P_{sat} = 26$  pW). Assuming a “safety factor” of 1.5 to reduce the risk of saturation, we adopt a target saturation power of  $P_{sat} = 45$  pW. The adopted safety factor results in an increase in system noise of 10 – 20% over BLIP for typical observing conditions and the assumed 65% optical efficiency. The adopted  $P_{sat}$  corresponds to an optical load of  $\sim 90$  K plus safety factor overhead.

If extra loading is present which saturates the detectors under an unacceptable range of observing conditions, the optical loading can be reduced by using a narrower bandpass filter or a neutral density filter. The resulting system sensitivity is close ( $< 10\%$ ) to what would be obtained had the system been designed for the higher loading.

Observing low-declination, early-summer targets will be difficult or impossible with the saturation power we have specified. For these cases we recommend providing for a reduction in the total throughput of the receiver via a warm neutral density filter and/or a more restrictive bandpass filter option.

Additional control over the loading and system noise may be provided by a remotely actuatable radome. Further investigation of this possibility is desirable.

#### References

- Mason & Perera 2010, GBT Memo 269, “The Effects of Weather on MUSTANG Data Quality”  
J.C. Mather 1982, Appl. Optics 21, 6  
J. R. Pardo, J. Cernicharo, and E. Serabyn ”Atmospheric Transmission at Microwaves (ATM): An Improved Model for mm/submm applications” IEEE Trans. on Antennas and Propagation, 49/12, 1683-1694 (2001)  
P.L. Richards 1994, J.Appl.Phys. 76, 1  
J.Sayers 2008, Ph.D. Thesis (California Institute of Technology)